Synthesis of Well-Ordered COF Monolayers: Surface Growth of Nanocrystalline Precursors *versus* Direct On-Surface Polycondensation

Jürgen F. Dienstmaier,[†,‡] Alexander M. Gigler,[‡] Andreas J. Goetz,[‡] Paul Knochel,[§] Thomas Bein,[§] Andrey Lyapin,[⊥] Stefan Reichlmaier,[⊥] Wolfgang M. Heckl,[†] and Markus Lackinger[†,*]

[†]Deutsches Museum, Museumsinsel 1, 80538 Munich, Germany, TUM School of Education, Technische Universität Munich, Schellingstrasse 33, 80799 Munich, Germany, and Center for NanoScience (CeNS), [‡]Department for Earth- and Environmental Sciences and Center for NanoScience (CeNS), Ludwig-Maximilians-University, Theresienstrasse 41, 80333 Munich, Germany, [§]Department of Chemistry and Center for NanoScience (CeNS), Ludwig-Maximilians-University, Butenandtstrasse 11 (E), 81377 Munich, Germany, and [⊥]Physical Electronics GmbH, Fraunhoferstr. 4, 85737 Ismaning, Germany

ABSTRACT Two different straightforward synthetic approaches are presented to fabricate long-range-ordered monolayers of a covalent organic framework (COF) on an inert, catalytically inactive graphite surface. Boronic acid condensation (dehydration) is employed as the polymerization reaction. In the first approach, the monomer is prepolymerized by a mere thermal treatment into nanocrystalline precursor COFs. The precursors are then deposited by drop-casting onto a graphite substrate and characterized by scanning tunneling microscopy (STM). While in the precursors monomers are already covalently interlinked into the final COF structure, the resulting domain size is still rather small. We show that a thermal treatment under reversible reaction conditions facilitates on-surface ripening associated with a striking increase of the domain size. Although this first approach allows studying different stages of the polymerization, the direct polymerization, that is, without the necessity of preceding reaction steps, is desirable. We demonstrate that even for a comparatively small diboronic acid monomer a direct thermally activated polymerization into extended COF monolayers is achievable.

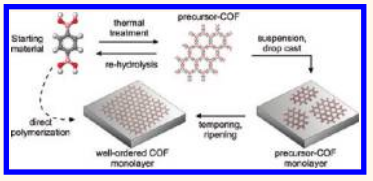

KEYWORDS: 2D COF · surface COF · COF-1 · boronic acid · condensation · STM · surface chemistry

Great chemical and structural variety of surface-supported two-dimensional porous molecular networks has been demonstrated over the past decade.[1,2] Formation and stabilization of porous monolayers can be mediated by various types of intermolecular interactions, most prominently by hydrogen bonding[3] and metal−ligand coordination,[4] but also by comparatively weak and nondirectional van der Waals interactions.[5] Owing to the weak to intermediate strength of these bond types, intermolecular links become reversible during network formation; hence, defect correction is possible and long-range-ordered structures are frequently obtained. Porous monolayers are highly interesting from a basic science perspective but also auspicious for nanotechnological applications, for instance, as nanoreactors for the synthesis of nanoparticles,[1] as templates for nanopatterning,[6] as well as for organic electronics.[7,8] However, many of the above applications or related processing steps demand higher stability of the networks, which ultimately leads to the requirement of strong intermolecular bonds, as realized in 2D polymers and covalent organic frameworks (COFs). Previously reported bulk COFs have been synthesized by various reactions such as self-condensation of boronic acids or co-condensation with polyols,[9,10] imine bond formation,[11] trimerization of nitriles,[12] and most recently, by means of hydrazine bond formation.[13] Bulk COFs have attracted considerable interest due to their porosity and low density in combination with the extraordinary stability of a covalent material. Moreover, COF structures can be tailored *via* rational design of appropriate building blocks.[9,10,14−19]

Similarly, the challenging synthesis of surface-supported covalent nanostructures and 2D COFs has recently gained substantial interest.[20] As polymerization reactions, radical addition,[21−27] condensation,[28−34] tip- and electron-beam-induced polymerization,[35] and alternative reactions[36−38] have been employed, first under ultrahigh vacuum (UHV) conditions, but meanwhile also under ambient conditions[39] or at the liquid−solid interface.[40]

* Address correspondence to markus@lackinger.org.

Received for review August 24, 2011 and accepted October 31, 2011.

Published online October 31, 2011
10.1021/nn2032616

Since most of the boronic-acid-derived bulk COFs exhibit a layered structure that consists of $\pi-\pi$ stacked covalent sheets, single layers of the corresponding bulk structure can serve as promising model systems for 2D COFs. The pioneering examples in this respect are the self-condensation of 1,4-benzenediboronic acid (BDBA) and the co-condensation of BDBA with 2,3,6,7,10,11-hexahydroxytriphenylene (HHTP) on Ag(111) under UHV conditions.[29] These experiments yielded monolayer equivalents of so-called COF-1 (self-condensation of BDBA) and COF-5 (co-condensation of BDBA + HHTP), whereby we refer to a nomenclature introduced by Yaghi and co-workers for bulk COFs.[9] However, nonreversible reaction conditions during the on-surface condensation polymerization resulted in high densities of topological defects that inhibited the emergence of long-range order as recently studied in more detail for different coinage metal surfaces and preparation conditions.[41] As an intermediate state between bulk crystals and monolayers, both COF-1 and COF-5 multilayers supported on a graphene substrate were recently demonstrated by a solvothermal approach.[42]

The objective of the present study is to explore the potential of straightforward synthetic approaches for the reliable and facile preparation of long-range-ordered surface-supported COF monolayers. In order to promote efficient synthesis, the proposed method is conducted under ambient conditions, hence does not require costly and time-consuming vacuum techniques, while it relies on reversible reaction conditions to facilitate long-range order. The targeted structure is a single layer of COF-1, synthesized by self-condensation of BDBA. Bulk crystals of COF-1 were first obtained by Yaghi and co-workers *via* solvothermal synthesis.[9] This approach avoids the "crystallization problem", that is, the absence of defect correction mechanisms during growth due to the irreversibility of covalent interlinks, by maintaining slightly reversible reaction conditions.[43,44] Self-condensation of boronic acids releases H_2O; consequently, the presence of small amounts of water in solution facilitates slightly reversible reaction conditions. A further aim of this study is to demonstrate polymerization on inert surfaces, in order to become independent of catalytic substrate properties, as they are indispensable for polymerization through radical addition.[45] Surface-mediated polymerization requires activation in order to break existent bonds and form new bonds. The self-condensation of boronic acids typically requires either reactive surfaces[29,41] or moderately elevated temperatures in the range of 80−100 °C as in the solvothermal synthesis. Yet, thermal activation can be crucial for on-surface reactions because desorption as a competing, likewise thermally activated, process may inhibit the surface-bound reaction. The BDBA monomer is comparatively small and features a low desorption barrier; hence, first a method is proposed where the monomers are prepolymerized into larger entities that already exhibit the COF-1 structure and owing to their size a larger desorption barrier. Although this approach allows control and characterization of single reaction steps, nonetheless, methods for direct polymerization, such as without intermediate reaction steps, are highly desirable. First we describe the prepolymerization of BDBA into nanocrystalline COF-1 precursors. Adsorbed monolayer structures are characterized in real space by high-resolution scanning tunneling microscopy (STM), whereas their covalent nature is independently verified by photoelectron spectroscopy and by demonstrating their thermal stability. In the last part, we also demonstrate a synthetic approach for the straightforward, direct polymerization of BDBA.

RESULTS AND DISCUSSION

The BDBA starting material and the reaction scheme are illustrated in Figure 1. Interestingly, ditopic BDBA monomers yield 2D covalently cross-linked sheets. The reason is the energetically preferred formation of boroxine rings (B_3O_3) through cyclocondensation of three monomers. In the 2D structure, both boronic acid groups of each BDBA monomer take part in boroxine rings, resulting in a hexagonal structure with *p6mm* symmetry and a lattice parameter of 1.525 nm, according to DFT geometry optimization.[29] COF-1-derived monolayers are porous and feature a hexagonal arrangement of approximately 1.0 nm wide pores.

Two different synthetic approaches are evaluated for the preparation of 2D COF-1 monolayers in this work. First, BDBA is prepolymerized into nanocrystalline COF-1 precursors, drop-cast on a graphite surface, and the domain size is increased by postprocessing. Second, a BDBA-containing solution is directly deposited onto the surface, and the condensation is thermally activated. The first synthetic approach allows one to carefully characterize important reaction parameters and intermediate states in order to understand fundamental processes in COF monolayer formation, whereas the second approach is straightforward and efficient for the routine preparation of 2D COF monolayers. In the following, we will describe the procedures for each synthesis route and the characterization of COF monolayers and intermediate states.

Synthesis *via* Prepolymerization into Nanocrystalline Precursor-COFs. COF-1 nanocrystals were synthesized by a mere thermal treatment of the BDBA starting material without any aid of solvent, yet under reversible reaction conditions (see Materials and Methods for experimental details). Thermally prepolymerized BDBA will be referred to as precursor-COF in the following. The prepolymerization was monitored by thermal gravimetric analysis (TGA), and COF-1 nanocrystals were characterized by powder X-ray diffraction (PXRD), IR,

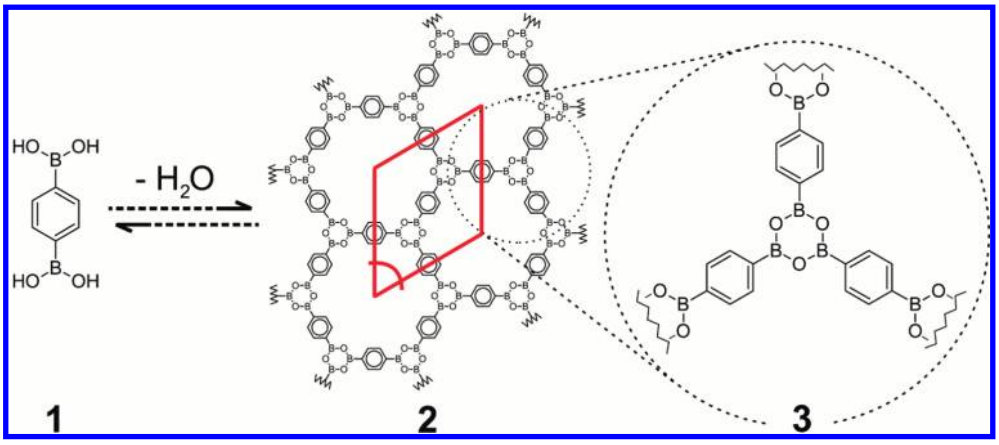

Figure 1. Reaction scheme for the self-condensation of BDBA from monomers (1) into single 2D COF-1 layers (2). During the condensation, H_2O is released, thus the presence of water facilitates reversible reaction conditions which promote growth of long-range-ordered networks. A unit cell of the 2D COF is marked by red lines, theoretical unit cell parameters from DFT geometry optimization of this hexagonal system amount to $a = b = 1.53$ nm and $\gamma = 60°$.[29] (3) Close-up of a boroxine ring resulting from the cyclocondensation of three BDBA monomers.

and Raman spectroscopy (see Supporting Information for data and spectra). Both Raman and IR spectra of thermally treated BDBA (*i.e.*, precursor-COFs) exhibit clear signatures of boroxine rings, while spectra of the untreated starting material clearly indicate free boronic acid groups. The IR spectra of precursor-COFs are also in excellent agreement with the results reported for solvothermally synthesized bulk COF-1.[9] PXRD exhibits rather broad reflections that are also consistent with the previously published COF-1 structure.[9] The large widths of the reflections originate from the finite sizes of COF-1 nanocrystals, while the presence of $l \neq 0$ reflections indicates stacking in the [001] direction, with a layer separation (*i.e.*, half the lattice parameter) of 0.335 nm. Estimates of the average crystal size were derived from a Rietveld refinement *via* the line broadening model based on the Scherrer equation and amount to 7.8 nm in the lateral direction and 1.0 nm along the [001] stacking direction, that is, about three single layers only (*cf.* Supporting Information).[46,47] In the TGA measurements, the weight loss sets in at ~150 °C and is 94% completed at 300 °C. The measured total weight loss of 20.4% is in good agreement with the theoretical expectation for full condensation (21.7%). The slight discrepancy might be caused by unreacted boronic acid groups at the surface of nanocrystals or by the presence of residual unreacted material. From these TGA results, we conclude that a prepolymerization temperature of 250 °C is well suited for thermal synthesis and should facilitate full condensation without degradation of precursor-COFs. The amount of residual unreacted BDBA after thermal treatment is extremely low, as characterized by means of a quartz crystal microbalance (*cf.* Supporting Information for details).

The full reversibility of the polycondensation is demonstrated through rehydrolizing the precursor-COFs by boiling them in distilled water and recrystallization.

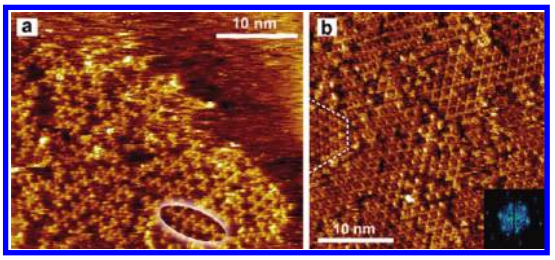

Figure 2. STM images of precursor-COFs on HOPG prepared by drop-casting of thermally treated BDBA, showing (a) chains that represent fragments of the COF-1 in-plane structure (a representative example is highlighted by the ellipse) and (b) 2D domains, with lateral extensions of typically <10 nm and internally hexagonal structure. The inset depicts the 2D FFT of the STM image. Both samples were prepared using heptanoic acid. The STM images were acquired at the liquid−solid interface with the tip immersed in the liquid. Most domains have similar azimuthal orientations, and an example for an occasionally observed exception is marked by dashed lines.

Data from all methods obtained with the rehydrolyzed precipitate were essentially similar to the untreated BDBA starting material, thereby proving the reversibility of the self-condensation reaction.

After thermal treatment, a small amount (~5 mg) of the prepolymerized precursor-COF was dispersed in 1.5 mL of various organic solvents (heptanoic acid, nonanoic acid, 1-undecanol, and dodecane). Experiments were conducted with different solvents in order to reveal possible solvent influences. Precursor-COFs were deposited by drop-casting 5 μL of the respective suspension onto a freshly cleaved surface of highly oriented pyrolytic graphite (HOPG). Structural characterization of the drop-cast layers was carried out under ambient conditions by high-resolution STM directly at the interface between the graphite substrate and the suspension. STM experiments reveal nearly full coverage of the surface. Predominantly chains and small domains of a hexagonal structure were observed on the surface; representative images are depicted in

Figure 2a,b. Areas between domain boundaries in Figure 2b are covered with smaller chain-like aggregates. The inset of Figure 2b depicts the corresponding 2D fast Fourier transform (2D FFT) of the image and clearly demonstrates the hexagonal symmetry of the domains. Averaging the values of about 40 independent images acquired with a thoroughly calibrated STM after drift and piezo creep have settled down yields lattice parameters of $a = b = 1.4 \pm 0.1$ nm and $\gamma = 60.0 \pm 2.5°$, which are in excellent agreement with both the in-plane lattice parameters reported for COF-1 (1.5 nm)[9] and with DFT values (1.525 nm) obtained for the 2D analogue.[29] However, boronic acids are also known to self-assemble *via* intermolecular hydrogen bonds.[48] In order to test the robustness of the postulated covalent structural model against competing noncovalent structures, a hypothetical hydrogen-bonded network was simulated by molecular mechanics (MM, *cf.* Supporting Information). Any reasonable structural model must fulfill the experimentally observed *p6mm* symmetry. In the STM data, connecting nodes between three molecules are clearly observed that would most likely be stabilized by cyclic hydrogen bonds in a noncovalent structure. However, the related MM geometry-optimized structure yields a significantly larger lattice parameter of 2.05 nm and can thus be excluded on experimental grounds. Similar STM experiments on drop-cast precursor-COF layers were carried out with different solvents, where comparable monolayers with similar hexagonal structure and lattice parameters were observed in heptanoic acid and nonanoic acid. However, no precursor-COF monolayers were observed in 1-undecanol and dodecane. These observations can be rationalized by the capability of the carboxylic acid moiety of the fatty acid solvents to stabilize the precursor-COFs in solution *via* strong hydrogen bonds with unreacted boronic acid groups that are prevalent at the edges. This additional favorable hydrogen bond stabilization is not as pronounced in 1-undecanol and entirely absent in the aprotic solvent dodecane, thereby lowering the achievable precursor-COF concentrations. Since usage of two different fatty acid solvents with different chain lengths did not affect the observed monolayer, solvent incorporation into the structures is excluded.

On the basis of careful analysis of structural parameters, we propose that the domains observed after drop-casting precursor-COF suspension are 2D covalent networks which structurally correspond to a single layer of COF-1. The STM image and the corresponding 2D FFT also indicate a preferred azimuthal orientation of the precursor-COF domains with respect to the underlying graphite lattice, pointing toward a substrate templating effect. In most images, a single orientation is prevalent, but domains with deviating azimuthal orientations are also observed occasionally; an example is marked in Figure 2b. This preferred epitaxial relation hints toward an extremely low thickness of the precursor-COF layer, and their uniform height, where steps have never been observed, indicates a spatially homogeneous thickness. In addition, the apparent height of the precursor-COF layer with respect to the bare graphite substrate as measured at domain boundaries corresponds to 0.30 ± 0.05 nm, which is extremely close to the geometric expectation. From these experimental observations, it is concluded that the STM measurements indeed show a single monolayer of precursor-COFs. However, STM imaging requires electrically conductive samples, and we can thus not fully exclude that the drop-cast deposition could also locally yield higher layer thicknesses, which is not observable by STM. We also note that the lateral extension of the domains below 10 nm in the STM data below 10 nm is consistent with the PXRD results on precursor-COFs.

In order to explore possibilities for increasing the domain size of the highly polycrystalline precursor-COF monolayers by postprocessing, samples were exposed to higher temperatures in a humid atmosphere (see Materials and Methods for details). Drop-cast samples were mounted in the reactor as prepared, that is, with remnants of the volatile solvents. Post-processed samples were characterized after cooling by ambient STM under dry conditions, without solvent on the samples; results are depicted in Figure 3. While the internal hexagonal structure is similar to the precursor-COF monolayer (*cf.* close-up and line profile in Figure 3b,c), a clear increase in domain size well above 40 nm is evident from the overview image. This can only be explained by on-surface ripening of the nanocrystalline precursor-COF domains. The apparent height of the 2D COF-1 adlayer with respect to the substrate as measured at domain boundaries corresponds to 0.30 ± 0.05 nm, proving that the STM observations indeed show a single monolayer of 2D COF-1. Also, the pores appear empty in the STM images, suggesting that residual solvent and monomers were entirely removed during the thermal treatment. While precursor-COF monolayers could only be imaged at the liquid–solid interface with heptanoic and nonanoic acid, extended COF-1 monolayers were also observed after thermal treatment using 1-undecanol and dodecane. This apparent contradiction can be explained by a low, but not vanishing, precursor-COF concentration in dodecane and 1-undecanol. Since the solvents completely evaporate at an early stage of the thermal treatment, all of the previously dispersed precursor-COFs in the entire solvent volume precipitate at the surface. Even so, the precursor-COF concentration in 1-undecanol and dodecane is too low to promote adsorption at the liquid–solid interface; it is apparently sufficient to feature COF monolayers after a thermal treatment.

Although the 2D COFs feature extremely low defect density, occasional point defects like missing building

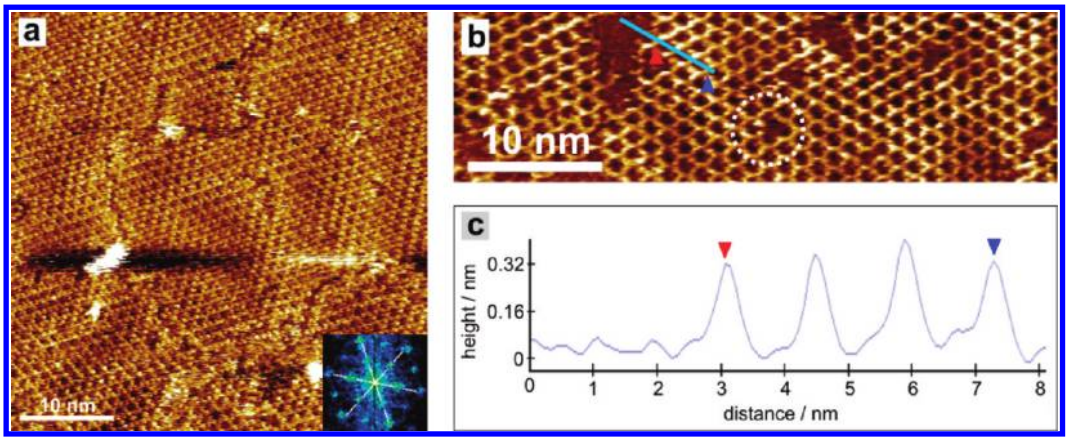

Figure 3. (a) STM image (acquired under dry conditions) of an extended 2D COF-1 monolayer. The sample was prepared by deposition of precursor-COFs from nonanoic acid and postprocessing by a thermal treatment. The inset depicts the corresponding 2D FFT of the image. The domain size is greatly increased as compared to the precursor-COF monolayer, and all domains in this image have similar azimuthal orientation. Point defects, like missing monomers, can be discerned with low density. The STM contrast also exhibits a nonperiodic height modulation. (b) High-resolution STM image of a 2D COF-1 monolayer on HOPG prepared similar as the sample in (a) but using heptanoic acid. Again, point defects like missing monomers can be discerned, and a prominent example is marked by the dashed circle. (c) Line profile along the blue line indicated in (b). The apparent height of the COF monolayer with respect to the uncovered substrate of ~0.30 nm indicates monolayer thickness, and the lattice parameter corresponds to 1.4 ± 0.1 nm.

blocks were also observed (*cf.* Figure 3a,b). It is noteworthy that the presence of water in the reactor is also extremely important for the on-surface ripening process. Postprocessing without adding water to the reactor did not result in an increase of the domain size but in a decrease of coverage due to the onset of desorption.

The contrast modulation discernible in Figures 3a, 4, and S2 (Supporting Information) is another interesting feature of the extended 2D COF monolayers. In general, STM contrast results from a convolution of electronic and geometric sample properties, and it can be difficult to discriminate between both. For instance, Moiré patterns are often observed in STM images of hydrogen-bonded organic monolayers on graphite[49,50] or graphene on HOPG and other substrates,[51−53] due to the higher (*i.e.*, over a larger integer number of lattice vectors) commensurability of adsorbate and superstructure lattice. However, Moiré patterns give rise to a periodic contrast modulation, whereas here the contrast modulation is not periodic. Whether this is a hint toward slight nonplanarity will be addressed in further experiments.

Additional Independent Evidence for Formation of COF-1 Monolayers. So far, the formation of COF-1 monolayers was concluded based on a comparison of STM-derived lattice parameters with experimental lattice parameters from bulk COF-1 and theoretical values from DFT calculations. Yet, verification of high thermal stability and photoelectron spectroscopy provide additional complementary evidence that actually covalent monolayers were formed.

In order to explore the thermal stability of these monolayers, postprocessed samples were exposed to a relatively high temperature of 200 °C for almost 14 h

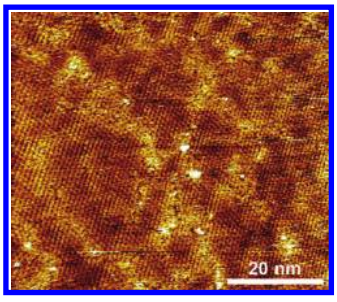

Figure 4. STM image (acquired under dry conditions) of an extended 2D COF-1 monolayer acquired under dry conditions. The sample was prepared by applying solutions of unreacted BDBA in nonanoic acid directly onto the substrate and thermal postprocessing under humid conditions. This sample is similar to the postprocessed precursor-COF monolayers with regard to lattice parameter, domain size, and defect density. Also, a nonperiodic contrast modulation is discernible here.

under ambient conditions and subsequently characterized by STM (*cf.* Supporting Information). Even after such rather harsh treatment for organic monolayers, hexagonal monolayers with similar lattice parameters could still be imaged by STM. If the monolayers were only stabilized by comparatively weak van der Waals interactions or even stronger hydrogen bonds, such a thermal treatment would result in desorption of the monolayer from the weakly interacting graphite substrate. As a reference, the thermal stability of trimesic acid (TMA) monolayers[54] that are stabilized by a fully cross-linked network of relatively strong double hydrogen bonds between carboxylic acid groups was studied by the same method. However, for this noncovalently stabilized TMA monolayer, annealing at 200 °C for 1 h already caused complete desorption. Consequently, the high thermal stability of the BDBA-derived monolayers can only be explained by formation of covalently interlinked networks. Yet, the

thermally treated COF-1 monolayers show a slight decrease in coverage, possibly hinting toward the onset of degradation.

In addition, the covalent character of the monolayers is also verified by comparative X-ray photoelectron spectra (XPS) that were acquired from both a thick film (>100 nm) of unreacted BDBA deposited by vacuum sublimation onto graphite and a postprocessed COF-1 monolayer. XPS data of O1s, B1s, and C1s core levels from both samples are depicted in Figure 5. Comparison reveals a slight shift of the O1s binding energy from 533.5 eV for the reference sample (unreacted BDBA) to 533.0 eV for the COF-1 monolayers. This slight shift toward lower binding energy for thermally treated samples is in accordance with the change of the oxygen chemical environment through condensation of boronic acid groups into boroxine rings and serves as further evidence for the polymerization. In the boronic acid moieties of unreacted BDBA monomers, oxygen is bound to both boron and hydrogen atoms, while in the boroxine rings of a COF-1 monolayer, oxygen is bound to two boron atoms. Since hydrogen is slightly more electronegative than boron (2.20 for H *vs* 2.04 for B on the Pauling scale), oxygen atoms become more negative in the boroxine rings, resulting in a slightly lower O1s binding energy in the COF-1 monolayer. Unfortunately, values for directly comparable compounds are not available in the literature, but for boron trioxide (B_2O_3), an O1s binding energy of 533.0 eV was reported,[55] whereas for boric acid ($B(OH)_3$), the O1s binding energy amounts to 533.5 eV.[56] As anticipated, both the B1s and C1s binding energies do not exhibit significant shifts because the direct binding partners of boron and carbon do not change through the condensation. The B1s peak at 191.7 eV coincides well with previously reported values for a chlorine-substituted phenyl boronic acid.[57] Yet, both intensity and line shape of the C1s peak are different between the BDBA film and COF monolayer: the BDBA film exhibits a symmetric main peak at 284.4 eV and a shakeup satellite at a higher binding energy of about 291 eV that is characteristic for aromatic molecules.[58,59] In the C1s spectrum of the COF-1 monolayer, this characteristic appearance is still discernible, but in addition, the signature from the graphite substrate with a narrow and asymmetric peak shape also contributes to the spectrum.[60]

Synthesis *via* Direct On-Surface Polymerization of BDBA. Introduction of precursor-COFs as the intermediate state for the synthesis of COF monolayers bears advantages for the fundamental understanding of the polymerization. For instance, we could show that on-surface ripening, that is, a significant increase in domain size, is feasible through thermal treatment under reversible reaction conditions. Also, additional analyses of IR and Raman spectroscopy could be applied to precursor-COFs but were inconclusive for monolayers. However, direct polymerization of the unreacted monomers on the surface would be advantageous in terms of easier and more efficient preparation protocols. In order to address the question, whether direct polycondensation of BDBA on the surface is also feasible, supersaturated BDBA solutions were directly deposited onto graphite and annealed in the reactor under humid conditions. Parameters for this thermal treatment were similar to the postprocessing of precursor-COF monolayers, and samples were again characterized by STM (*cf.* Supporting Information). STM data of directly polymerized COF-1 monolayers were indistinguishable from monolayers that were fabricated *via* ripening of drop-cast precursor-COFs. Not only lattice parameters were similar, but also domain size and point defect density were comparable. Similarly, a nonperiodic height modulation on the 10 nm length scale is again pointing toward a slightly nonplanar character. As an independent proof of the covalent nature of directly prepared COF-1 monolayers, their thermal stability was verified according to the previous procedure. Direct BDBA polymerization was also accomplished in different aliphatic solvents (heptanoic acid, nonanoic acid, 1-undecanol, and dodecane), suggesting a minor solvent influence. Experiments with different BDBA concentrations in nonanoic acid clearly show that the direct polymerization is only possible at higher concentrations (*i.e.*, supersaturations).

In summary, we demonstrate that even when the BDBA monomers were not prepolymerized into larger entities, their thermally activated polymerization is feasible and yields similar results as on-surface ripening of precursor-COF monolayers. From these experiments, we conclude that either desorption is not the dominating thermally activated process or is suppressed in the critical stage of the polycondensation. Hence, direct polymerization of the ditopic boronic acid linker is the most straightforward method for the reliable and efficient preparation of extended, well-ordered COF-1 monolayers under ambient conditions.

CONCLUSION AND OUTLOOK

In summary, we have demonstrated the potential of straightforward synthetic approaches to prepare surface-confined 2D COFs with single-crystalline domains having lateral extensions above 40 nm. In a first synthetic route, nanocrystalline precursor-COFs were synthesized by thermally annealing the bisboronic acid building blocks in a humid atmosphere, drop-cast deposition of a monolayer, and a thermally activated ripening of initially very small domains into extended domains. The covalent nature of the network was proven by comparison of experimental structural parameters with DFT calculations, augmented by XPS and verification of the anticipated high stability

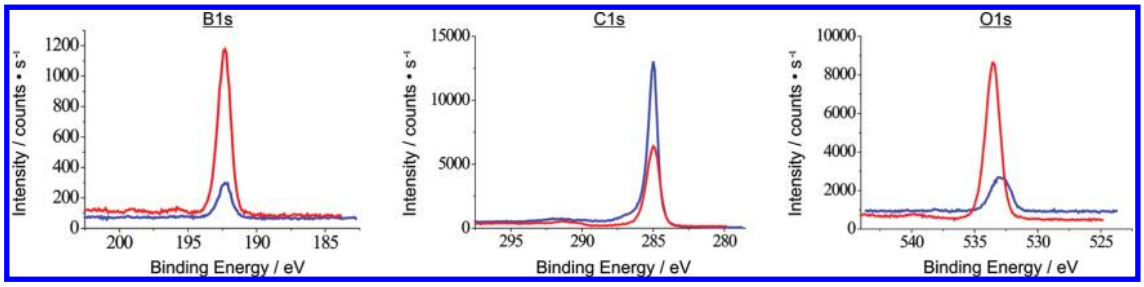

Figure 5. XPS measurements of the B1s, C1s, and O1s core level binding energies in a thick BDBA film on HOPG (red) and a 2D COF-1 monolayer on HOPG (blue). O1s spectra of the polymerized 2D COF-1 monolayer exhibit a slight shift to lower binding energy as compared to the film of unreacted BDBA molecules. This can be explained by the change of the oxygen chemical environment from B−O−H in the free boronic acid group to B−O−B in the boroxine ring upon condensation. Both the B1s and C1s spectra do not exhibit any significant shifts because their direct chemical environments are not affected by the condensation reaction. The high intensity of C1s in the COF-1 monolayer sample originates from the HOPG substrate.

through a thermal treatment. While this stepwise synthesis allows one to characterize reaction intermediates and to demonstrate that on-surface ripening of COF-1 monolayers is possible, the controllable direct synthesis from not previously treated monomers would facilitate significantly easier preparation protocols. We show that a direct polymerization is also feasible, by deposition of a solution containing the unreacted BDBA monomer and a thermal treatment under reversible reaction conditions. COF-1 monolayers prepared by either method were indistinguishable in STM measurements and both exhibit high thermal stability.

The novel synthetic approaches presented here avoid elaborate vacuum deposition techniques and should in principle be scalable to larger surface areas. As for solvothermal methods, the presence of water is important for the polycondensation of BDBA in both the direct synthesis and the stepwise synthesis *via* prepolymerization and ripening, in order to facilitate the slight reversibility required for successful crystallization. While the proposed synthetic approaches are facile and reliable, the next challenge is to adapt the preparation protocol to accomplish structural versatility. Here, the proof of principle has been demonstrated by means of a relatively simple one-component system. Significantly greater structural and chemical diversity can be achieved, however, by combining two building blocks as demonstrated for the solvothermal synthesis of several bulk COFs. Thus, adaptation of the proposed method to the combination of several more complex building blocks is the next important step.

MATERIALS AND METHODS

Thermal Synthesis of Nanocrystalline Precursor-COFs. BDBA (Sigma-Aldrich, 98.1% purity) was used without further purification. For the thermally induced polymerization, a small amount of BDBA (~0.2 g) was exposed to a temperature of 250 °C for 2 h in a preheated oven (volume = 4.3 L) under ambient conditions. Thereafter, the powdery product was removed and allowed to cool to room temperature without special precautions. An additional crucible with water (~65 mL) in the oven guaranteed a high humidity throughout the process. Similar thermal treatment of BDBA in a dry atmosphere yielded only small aggregates that were not suited for further processing (*cf.* Supporting Information). We find that the solvent-free condensation does not require exact adjustment of the H_2O partial pressure during the thermal treatment, as long as water is present at all. The powdery product obtained after the prepolymerization has a slight yellowish tinge, presumably due to char formation or unexpected reactions with impurities.[61] Different organic solvents were used both for BDBA monomers and precursor-COFs: heptanoic acid (Fluka, purity ≥98%), nonanoic acid (SAFC, purity ≥96%), 1-undecanol (Aldrich, purity 99%), and dodecane (Sigma-Aldrich, anhydrous, purity ≥99%).

Postprocessing of Precursor-COF Monolayers. Drop-cast samples were positioned inside a stainless steel reactor (7.7 cm^3) that was placed in a preheated oven at 120 °C for ~60 min. Samples were mounted face down, and 50−100 μL of H_2O were added to the bottom of the reactor, but not in direct contact with the sample. Varying the amount of water in this range does not have any observable effect on the final structures. The reactor can be sealed off with a valve (Swagelok, SS Bellows sealed valve), which was, however, kept slightly open during the postprocessing to allow gas exchange with the ambient environment and to ensure that the interior always remained at atmospheric pressure. In this experiment, the precise moment of complete disappearance of the liquid water is not known. We anticipate that when water is not present anymore, bond reversibility and thus domain ripening come to an end. In order to track the temperature during cooling and heating times, the temperature inside the reactor was monitored with a thermocouple. The maximum temperature in the 60 min period was 107 °C; a full temperature profile is reproduced in the Supporting Information.

Analytics. Raman spectra were acquired with a confocal Raman microscope (alpha300 R; WITec GmbH, Ulm, Germany) using excitation at λ = 785 nm. Single spectra were acquired at several positions on each sample averaging 10 spectra with 5 s integration time each at a laser power of 50 mW. For optimum signal efficiency, a 100× microscope objective with a numerical aperture of 0.9 was used. IR spectra were acquired with a Bruker Equinox 55 instrument. Small amounts of the samples (untreated, thermally treated, and rehydrolyzed BDBA) were mixed with dry KBr (previously dehydrated for ~1 week), compressed into pellets, and immediately analyzed. TGA was performed with a Netzsch STA 449 C instrument, with a heating rate of 10 °C/s and an original weight of 11.4 mg of BDBA. PXRD characterization was performed on an Oxford Diffraction diffractometer equipped with a 2D Atlas detector, operating at 100 mm sample to detector distance and using Mo $K_{\alpha 1}$ radiation (HOPG monochromator). The data obtained by recording several frames of Debye−Scherrer rings on the 2D detector were integrated to one-dimensional intensity *versus* 2Θ data by the

diffractometer software (CRYSALIS PRO). The scattering from the mylar foil and the instrumental background were subtracted during the postprocessing. General Structure Analysis System (GSAS) software with the graphical front-end EXPGUI was used for the estimation of the coherent domain size *via* an anisotropic line broadening model using the Scherrer equation.[46,47] In nanocrystalline materials, the coherent domain size can be assumed to be equal to the crystallite size. The previously reported structure of COF-1 was used as a model.[9] The atomic positions were fixed during the simulation, and texture effects were corrected with a March-Dollase model assuming a preferred orientation of 0.5 for 001. The final χ^2 distribution was found to be 3.145.

STM images were acquired with a home-built drift-stable scanning probe microscope operated by an ASC500 scanning probe microscopy controller from attocube systems AG. STM measurements were conducted either directly at the liquid−solid interface (precursor-COF monolayer) or under dry conditions (after postprocessing). Constant current images were obtained with tunneling voltages between +0.3 and +0.9 V applied to the tip and set point currents between 50 and 90 pA.

XPS analysis was performed with a PHI 5000 VersaProbe spectrometer (Physical Electronics) equipped with a 180° spherical energy analyzer and a multichannel detection system with 16 channels. Spectra were acquired at a base pressure of 5×10^{-7} Pa using a focused scanning monochromatic Al K_α source (1486.68 eV) with spot size of 200 μm and beam power of 50 W. The instrument was run in the FAT analyzer mode with electrons emitted at 45° to the surface normal. Dual beam charge neutralization was applied throughout the analysis. High-resolution scans of the B1s, C1s, and O1s energy spectra were taken with a pass energy of 23.5 eV. Data were analyzed using the program MultiPak.

Acknowledgment. Financial support from the Nano Systems Initiative Munich (NIM) and the Bayerische Forschungsstiftung is gratefully acknowledged. We also would like to thank WITec GmbH for granting the Raman measurements, Johanna Eichhorn, Dr. Kai-Uwe Hess for their assistance with effusion cell BDBA deposition rates and TGA measurements, and Prof. Stefan Sotier for initial XPS measurements.

Supporting Information Available: Additional STM images, PXRD, IR, Raman, TGA data, sublimation curves for BDBA, molecular mechanics simulation of hypothetical self-assembled BDBA monolayers, and temperature profile inside the reactor during the thermal activation. This material is available free of charge *via* the Internet at http://pubs.acs.org.

REFERENCES AND NOTES

1. Lei, S. B.; Tahara, K.; Adisoejoso, J.; Balandina, T.; Tobe, Y.; De Feyter, S. Towards Two-Dimensional Nanoporous Networks: Crystal Engineering at the Solid−Liquid Interface. *CrystEngComm* **2010**, *12*, 3369–3381.
2. De Feyter, S.; Elemans, J. A. A. W.; Lei, S. B. Molecular and Supramolecular Networks on Surfaces: From Two-Dimensional Crystal Engineering to Reactivity. *Angew. Chem., Int. Ed.* **2009**, *48*, 7298–7332.
3. Lackinger, M.; Griessl, S.; Heckl, W. M.; Hietschold, M.; Flynn, G. W. Self-Assembly of Trimesic Acid at the Liquid−Solid Interface—A Study of Solvent-Induced Polymorphism. *Langmuir* **2005**, *21*, 4984–4988.
4. Shi, Z.; Lin, N. Porphyrin-Based Two-Dimensional Coordination Kagome Lattice Self-Assembled on a Au(111) Surface. *J. Am. Chem. Soc.* **2009**, *131*, 5376–5377.
5. Lei, S.; Tahara, K.; De Schryver, F. C.; Van der Auweraer, M.; Tobe, Y.; De Feyter, S. One Building Block, Two Different Supramolecular Surface-Confined Patterns: Concentration in Control at the Solid−Liquid Interface. *Angew. Chem., Int. Ed.* **2008**, *47*, 2964–2968.
6. Joo, S. H.; Choi, S. J.; Oh, I.; Kwak, J.; Liu, Z.; Terasaki, O.; Ryoo, R. Ordered Nanoporous Arrays of Carbon Supporting High Dispersions of Platinum Nanoparticles. *Nature* **2001**, *412*, 169–172.
7. Spitler, E. L.; Dichtel, W. R. Lewis Acid-Catalysed Formation of Two-Dimensional Phthalocyanine Covalent Organic Frameworks. *Nat. Chem.* **2010**, *2*, 672–677.
8. Jiang, D. L.; Wan, S.; Guo, J.; Kim, J.; Ihee, H. A Belt-Shaped Blue Luminescent, and Semiconducting Covalent Organic Framework. *Angew. Chem., Int. Ed.* **2008**, *47*, 8826–8830.
9. Cote, A. P.; Benin, A. I.; Ockwig, N. W.; O'Keeffe, M.; Matzger, A. J.; Yaghi, O. M. Porous, Crystalline, Covalent Organic Frameworks. *Science* **2005**, *310*, 1166–1170.
10. Cote, A. P.; El-Kaderi, H. M.; Furukawa, H.; Hunt, J. R.; Yaghi, O. M. Reticular Synthesis of Microporous and Mesoporous 2D Covalent Organic Frameworks. *J. Am. Chem. Soc.* **2007**, *129*, 12914–12915.
11. Uribe-Romo, F. J.; Hunt, J. R.; Furukawa, H.; Klock, C.; O'Keeffe, M.; Yaghi, O. M. A Crystalline Imine-Linked 3-D Porous Covalent Organic Framework. *J. Am. Chem. Soc.* **2009**, *131*, 4570–4571.
12. Kuhn, P.; Antonietti, M.; Thomas, A. Porous, Covalent Triazine-Based Frameworks Prepared by Ionothermal Synthesis. *Angew. Chem., Int. Ed.* **2008**, *47*, 3450–3453.
13. Uribe-Romo, F. J.; Doonan, C. J.; Furukawa, H.; Oisaki, K.; Yaghi, O. M. Crystalline Covalent Organic Frameworks with Hydrazone Linkages. *J. Am. Chem. Soc.* **2011**, *133*, 11478–11481.
14. Korich, A. L.; Iovine, P. M. Boroxine Chemistry and Applications: A Perspective. *Dalton Trans.* **2010**, *39*, 1423–1431.
15. Nishiyabu, R.; Kubo, Y.; James, T. D.; Fossey, J. S. Boronic Acid Building Blocks: Tools for Self Assembly. *Chem. Commun.* **2011**, *47*, 1124–1150.
16. Tilford, R. W.; Gemmill, W. R.; zur Loye, H. C.; Lavigne, J. J. Facile Synthesis of a Highly Crystalline, Covalently Linked Porous Boronate Network. *Chem. Mater.* **2006**, *18*, 5296–5301.
17. El-Kaderi, H. M.; Hunt, J. R.; Mendoza-Cortes, J. L.; Cote, A. P.; Taylor, R. E.; O'Keeffe, M.; Yaghi, O. M. Designed Synthesis of 3D Covalent Organic Frameworks. *Science* **2007**, *316*, 268–272.
18. Campbell, N. L.; Clowes, R.; Ritchie, L. K.; Cooper, A. I. Rapid Microwave Synthesis and Purification of Porous Covalent Organic Frameworks. *Chem. Mater.* **2009**, *21*, 204–206.
19. Wan, S.; Guo, J.; Kim, J.; Ihee, H.; Jiang, D. A Photoconductive Covalent Organic Framework: Self-Condensed Arene Cubes Composed of Eclipsed 2D Polypyrene Sheets for Photocurrent Generation. *Angew. Chem., Int. Ed.* **2009**, *48*, 5439–5442.
20. Sakamoto, J.; van Heijst, J.; Lukin, O.; Schluter, A. D. Two-Dimensional Polymers: Just a Dream of Synthetic Chemists? *Angew. Chem., Int. Ed.* **2009**, *48*, 1030–1069.
21. Bieri, M.; Blankenburg, S.; Kivala, M.; Pignedoli, C. A.; Ruffieux, P.; Müllen, K.; Fasel, R. Surface-Supported 2D Heterotriangulene Polymers. *Chem. Commun.* **2011**, *47*, 10239–10241.
22. Blunt, M. O.; Russell, J. C.; Champness, N. R.; Beton, P. H. Templating Molecular Adsorption Using a Covalent Organic Framework. *Chem. Commun.* **2010**, *46*, 7157–7159.
23. Grill, L.; Dyer, M.; Lafferentz, L.; Persson, M.; Peters, M. V.; Hecht, S. Nano-architectures by Covalent Assembly of Molecular Building Blocks. *Nat. Nanotechnol.* **2007**, *2*, 687–691.
24. Gutzler, R.; Walch, H.; Eder, G.; Kloft, S.; Heckl, W. M.; Lackinger, M. Surface Mediated Synthesis of 2D Covalent Organic Frameworks: 1,3,5-Tris(4-bromophenyl)benzene on Graphite(001), Cu(111), and Ag(110). *Chem. Commun.* **2009**, 4456–4458.
25. Cai, J.; Ruffieux, P.; Jaafar, R.; Bieri, M.; Braun, T.; Blankenburg, S.; Muoth, M.; Seitsonen, A. P.; Saleh, M.; Feng, X.; Müllen, K.; Fasel, R. Atomically Precise Bottom-Up Fabrication of Graphene Nanoribbons. *Nature* **2010**, *466*, 470–473.
26. Lipton-Duffin, J. A.; Ivasenko, O.; Perepichka, D. F.; Rosei, F. Synthesis of Polyphenylene Molecular Wires by Surface-Confined Polymerization. *Small* **2009**, *5*, 592–597.
27. Lipton-Duffin, J. A.; Miwa, J. A.; Kondratenko, M.; Cicoira, F.; Sumpter, B. G.; Meunier, V.; Perepichka, D. F.; Rosei, F. Step-by-Step Growth of Epitaxially Aligned Polythiophene by Surface-Confined Reaction. *Proc. Natl. Acad. Sci. U.S.A.* **2010**.

28. Schmitz, C. H.; Schmid, M.; Gärtner, S.; Steinrück, H.-P.; Gottfried, J. M.; Sokolowski, M. Surface Polymerization of Poly(*p*-phenylene-terephthalamide) on Ag(111) Investigated by X-ray Photoelectron Spectroscopy and Scanning Tunneling Microscopy. *J. Phys. Chem. C* **2011**, *115*, 18186–18194.
29. Zwaneveld, N. A. A.; Pawlak, R.; Abel, M.; Catalin, D.; Gigmes, D.; Bertin, D.; Porte, L. Organized Formation of 2D Extended Covalent Organic Frameworks at Surfaces. *J. Am. Chem. Soc.* **2008**, *130*, 6678–6679.
30. Treier, M.; Richardson, N. V.; Fasel, R. Fabrication of Surface-Supported Low-Dimensional Polyimide Networks. *J. Am. Chem. Soc.* **2008**, *130*, 14054–14055.
31. Jensen, S.; Greenwood, J.; Früchtl, H. A.; Baddeley, C. J. STM Investigation on the Formation of Oligoamides on Au{111} by Surface-Confined Reactions of Melamine with Trimesoyl Chloride. *J. Phy. Chem. C* **2011**, *115*, 8630–8636.
32. Schmitz, C. H.; Ikonomov, J.; Sokolowski, M. Two-Dimensional Polyamide Networks with a Broad Pore Size Distribution on the Ag(111) Surface. *J. Phys. Chem. C* **2011**, *115*, 7270–7278.
33. Weigelt, S.; Busse, C.; Bombis, C.; Knudsen, M. M.; Gothelf, K. V.; Lægsgaard, E.; Besenbacher, F.; Linderoth, T. R. Surface Synthesis of 2D Branched Polymer Nanostructures. *Angew. Chem., Int. Ed.* **2008**, *47*, 4406–4410.
34. Treier, M.; Fasel, R.; Champness, N. R.; Argent, S.; Richardson, N. V. Molecular Imaging of Polyimide Formation. *Phys. Chem. Chem. Phys.* **2009**, *11*, 1209–1214.
35. Clair, S.; Ourdjini, O.; Abel, M.; Porte, L. Tip- or Electron Beam-Induced Surface Polymerization. *Chem. Commun.* **2011**, *47*, 8028–8030.
36. Abel, M.; Clair, S.; Ourdjini, O.; Mossoyan, M.; Porte, L. Single Layer of Polymeric Fe-Phthalocyanine: An Organometallic Sheet on Metal and Thin Insulating Film. *J. Am. Chem. Soc.* **2011**, *133*, 1203–1205.
37. In't Veld, M.; Iavicoli, P.; Haq, S.; Amabilino, D. B.; Raval, R. Unique Intermolecular Reaction of Simple Porphyrins at a Metal Surface Gives Covalent Nanostructures. *Chem. Commun.* **2008**, 1536–1538.
38. Matena, M.; Riehm, T.; Stöhr, M.; Jung, T. A.; Gade, L. H. Transforming Surface Coordination Polymers into Covalent Surface Polymers: Linked Polycondensed Aromatics through Oligomerization of N-Heterocyclic Carbene Intermediates. *Angew. Chem., Int. Ed.* **2008**, *47*, 2414–2417.
39. Beton, P. H.; Russell, J. C.; Blunt, M. O.; Garfitt, J. M.; Scurr, D. J.; Alexander, M.; Champness, N. R. Dimerization of Tri(4-bromophenyl)benzene by Aryl−Aryl Coupling from Solution on a Gold Surface. *J. Am. Chem. Soc.* **2011**, *133*, 4220–4223.
40. Tanoue, R.; Higuchi, R.; Enoki, N.; Miyasato, Y.; Uemura, S.; Kimizuka, N.; Stieg, A. Z.; Gimzewski, J. K.; Kunitake, M. Thermodynamically Controlled Self-Assembly of Covalent Nanoarchitectures in Aqueous Solution. *ACS Nano* **2011**, *5*, 3923–3929.
41. Ourdjini, O.; Pawlak, R.; Abel, M.; Clair, S.; Chen, L.; Bergeon, N.; Sassi, M.; Oison, V.; Debierre, J.-M.; Coratger, R.; Porte, L. Substrate-Mediated Ordering and Defect Analysis of a Surface Covalent Organic Framework. *Phys. Rev. B* **2011**, *84*, 125421.
42. Colson, J. W.; Woll, A. R.; Mukherjee, A.; Levendorf, M. P.; Spitler, E. L.; Shields, V. B.; Spencer, M. G.; Park, J.; Dichtel, W. R. Oriented 2D Covalent Organic Framework Thin Films on Single-Layer Graphene. *Science* **2011**, *332*, 228–231.
43. Whitesides, G. M.; Grzybowski, B. Self-Assembly at All Scales. *Science* **2002**, *295*, 2418–2421.
44. Perepichka, D. F.; Rosei, F. Extending Polymer Conjugation into the Second Dimension. *Science* **2009**, *323*, 216–217.
45. Walch, H.; Gutzler, R.; Sirtl, T.; Eder, G.; Lackinger, M. Material- and Orientation-Dependent Reactivity for Heterogeneously Catalyzed Carbon−Bromine Bond Homolysis. *J. Phys. Chem. C* **2010**, *114*, 12604–12609.
46. Larson, A. C.; von Dreele, R. B. *General Structure Analysis System* (GSAS), Los Alamos National Laboratory Report LAUR 86-748, 2000.
47. Toby, B. H. EXPGUI, a Graphical User Interface for GSAS. *J. Appl. Crystallogr.* **2001**, *34*, 210–213.
48. Pawlak, R.; Nony, L.; Bocquet, F.; Olson, V.; Sassi, M.; Debierre, J. M.; Loppacher, C.; Porte, L. Supramolecular Assemblies of 1,4-Benzene Diboronic Acid on KCl(001). *J. Phys. Chem. C* **2010**, *114*, 9290–9295.
49. Edelwirth, M.; Freund, J.; Sowerby, S. J.; Heckl, W. M. Molecular Mechanics Study of Hydrogen Bonded Self-Assembled Adenine Monolayers on Graphite. *Surf. Sci.* **1998**, *417*, 201–209.
50. Thomas, L. K.; Kühnle, A.; Rode, S.; Beginn, U.; Reichling, M. Monolayer Structure of Arachidic Acid on Graphite. *J. Phys. Chem. C* **2010**, *114*, 18919–18924.
51. Zhang, J. F.; Cao, G. Y. STM Study of Moiré Patterns on HOPG. *Chin. J. Chem. Phys.* **2006**, *19*, 197–199.
52. Xhie, J.; Sattler, K.; Ge, M.; Venkateswaran, N. Giant and Supergiant Lattices on Graphite. *Phys. Rev. B* **1993**, *47*, 15835–15841.
53. Wang, B.; Bocquet, M. L.; Marchini, S.; Günther, S.; Wintterlin, J. Chemical Origin of a Graphene Moiré Overlayer on Ru(0001). *Phys. Chem. Chem. Phys.* **2008**, *10*, 3530–3534.
54. Griessl, S.; Lackinger, M.; Edelwirth, M.; Hietschold, M.; Heckl, W. M. Self-Assembled Two-Dimensional Molecular Host−Guest Architectures from Trimesic Acid. *Single Mol.* **2002**, *3*, 25–31.
55. Nefedov, V. I.; Gati, D.; Dzhurinskii, B. F.; Sergushin, N. P.; Salyn, Y. V. The X-ray Electronic Studies of Oxides of Certain Elements. *Z. Neorg. Khim.* **1975**, *20*, 2307–2314.
56. Brian, R, S. Surface Characterization of Aluminum Foil Annealed in the Presence of Ammonium Fluoborate. *Appl. Surf. Sci.* **1989**, *40*, 249–263.
57. Hendrickson, D. N.; Hollander, J. M.; Jolly, W. L. Core-Electron Binding Energies for Compounds of Boron, Carbon, and Chromium. *Inorg. Chem.* **1970**, *9*, 612–615.
58. Jones, T. S.; Ashton, M. R.; Richardson, N. V.; Mack, R. G.; Unertl, W. N. The Interaction of the Polyimide Precursors PMDA (1,2,4,5-Benzenetetracarboxylic Anhydride) and m-PDA (1,3-Phenylenediamine) with Ni(110). *J. Vac. Sci. Technol., A* **1990**, *8*, 2370–2375.
59. Keane, M. P.; de Brito, A. N.; Correia, N.; Svensson, S.; Lunell, S. Experimental and Theoretical Study of the N1s and C1s Shake-Up Satellites in Pyridine and Aniline. *Chem. Phys.* **1991**, *155*, 379–387.
60. van Attekum, P. M. T. M.; Wertheim, G. K. Excitonic Effects in Core-Hole Screening. *Phys. Rev. Lett.* **1979**, *43*, 1896–1898.
61. Morgan, A. B.; Jurs, J. L.; Tour, J. M. Synthesis, Flame-Retardancy Testing, and Preliminary Mechanism Studies of Nonhalogenated Aromatic Boronic Acids: A New Class of Condensed-Phase Polymer Flame-Retardant Additives for Acrylonitrile-Butadiene-Styrene and Polycarbonate. *J. Appl. Polym. Sci.* **2000**, *76*, 1257–1268.